arXiv:2606.26502v4 [cs.AI] 8 Sep 2026

Humans Disengage, Reasoning Models Persist
Separating Difficulty Registration from Deliberation Allocation

Han-yu Wang
The University of Hong Kong
henry.why@connect.hku.hk

Abstract

Large reasoning models (LRMs) tend to produce longer reasoning traces for problems on which humans also spend more time. This correspondence suggests a shared sensitivity to difficulty, yet difficult problems can invite both persistence and withdrawal. We distinguish difficulty registration, expressed in which problems elicit more deliberation, from the allocation of further work. We examine their relation in matched human and LRM data from visual abstraction, intuitive physics, and relational reasoning. On visual abstraction, model trace length tracks the human ordering of problems by duration. After item identity is controlled, successful human attempts last longer than failed attempts, while failed LRM attempts have longer traces than successful ones in the pooled model analysis. The estimated outcome slopes follow the same pattern in intuitive physics. In relational reasoning, successful attempts are longer in separate human and model analyses. Fitting the two groups together with shared item effects yields a human-LRM difference in the relation between duration and outcome. Human grid actions connect longer attempts with sustained task engagement. Failed LRM traces contain more hedging or repetition after length is controlled, with the form of the difference varying across tasks. A resource-rational account explains how the expected reducibility of uncertainty and the value assigned to further computation can produce different patterns of persistence despite similar sensitivity to difficulty. Agreement about which problems require more deliberation can therefore coexist with different patterns of persistence on those problems.

Keywords large reasoning models, deliberation, reaction time, chain-of-thought, resource-rational analysis

1 Introduction

Research on deliberation asks how a cognitive system decides whether further thought is worth its cost. Sequential-sampling models distinguish an evolving evidence state from the stopping rule applied to it (Ratcliff and McKoon, 2008, Bogacz et al., 2006, Heitz, 2014). Metacognitive theories distinguish monitoring of confidence or uncertainty from the control of continued effort (Nelson and Narens, 1990, Yeung and Summerfield, 2012, Nelson and Leonesio, 1988). Resource-rational metareasoning asks whether another computation promises enough improvement to justify its opportunity cost (Simon, 1956, Russell and Wefald, 1991, Lieder and Griffiths, 2020, Gershman et al., 2015, Callaway et al., 2022). Each account distinguishes information about the current state from the rule that determines whether work continues, stops, or changes direction.

Further thought can remain worthwhile on a difficult problem if continued search still seems promising. The same difficulty can also prompt withdrawal when progress seems unlikely, or a change of approach when the current route loses value. We use *difficulty registration* for sensitivity

to differences in problem difficulty, expressed in observable deliberation, and *deliberation allocation* for how an agent distributes further work once difficulty is encountered. Two agents can register a similar ordering of difficult problems and differ in when they persist.

We examine these relations through the duration of individual attempts. Across problems, we ask whether the same items elicit more deliberation from each system. Among attempts on the same problem, we ask how duration differs between those that eventually succeed and those that fail.

Large reasoning models (LRMs) make this comparison possible because they generate intermediate reasoning traces before a final answer (Wei et al., 2022, Kojima et al., 2022, Snell et al., 2025). Such behavioural signatures are increasingly used to study their relation to human cognition (Binz and Schulz, 2023). de Varda et al. (2025) reported that LRM reasoning-token length tracks human reaction time across seven reasoning tasks. Problems that take humans longer also tend to elicit longer model traces. Although seconds and tokens measure different activities, their cross-problem correlation reveals a correspondence in the relative duration devoted to particular items. The question is how far this correspondence extends to continued work once difficulty has been encountered.

Two agents can share a cross-problem ordering even if one abandons some difficult attempts quickly and the other continues searching until they end in error. Both may spend longer on difficult problems overall. A correlation across items leaves this difference unresolved because item difficulty and persistence contribute to the same duration measure. Comparing successful and failed attempts after item identity is held fixed separates the shared difficulty gradient from this further source of variation.

Recent discussion of reasoning traces has focused on what their length represents. Vankov et al. (2026) found little accuracy change under reasoning-effort manipulations in five of six tasks and questioned a causal interpretation of trace length. Dujmović (2026) argued that behavioural correlation alone does not establish mechanistic similarity. Hu (2026) proposed that intermediate tokens may function as performative scaffolding and suggested inference-time truncation as a test of their incremental contribution to performance. Replies defend the cross-problem regularity while leaving its algorithmic explanation open (de Varda et al., 2026a,b). Allocation raises a further behavioural question within this debate. Do humans and LRMs concentrate continued deliberation in the same kinds of trajectories when they encounter difficult problems?

We examine this question in three reasoning paradigms. H-ARC provides the primary test in visual abstraction, INTUIT extends the comparison to intuitive physics, and Cortes tests binary relational reasoning. The sample contains six open-weight thinking LRMs and DeepSeek-V3 as a non-thinking baseline. We first compare duration on successful and failed trials within each agent, then estimate human and LRM outcome slopes with item fixed effects. Human grid actions and model trace content show what participants do and what models generate during longer attempts. The paradigms vary in search structure and answer space, allowing us to ask whether the human-LRM difference extends across tasks and whether it always takes the form of opposite outcome slopes. By examining both registration and allocation, we locate similarity in sensitivity to difficulty and test how far it extends to deliberative control.

2 Methods

Data and deliberation measures. This study reanalyses publicly released, de-identified human and LRM data from the de Varda et al. (2025) release and the underlying behavioural corpora (LeGris et al., 2025, Prunty et al., 2025, Cortés et al., 2021). No new human-subjects data were

collected. Table 1 summarises the paradigms. H-ARC (LeGris et al., 2025, Chollet, 2019) tests visual abstraction, INTUIT tests intuitive physics, and Cortes tests binary relational reasoning. Arithmetic is excluded because all thinking LRMs are at ceiling.

The thinking-LRM sample consists of models that expose an intermediate reasoning trace. It includes DeepSeek-R1 (Guo et al., 2025), Qwen-QwQ-32B and Qwen3-235B-Thinking (Qwen Team, 2025), GLM-4.5-Air-FP8 (Z.ai, 2025), and gpt-oss-20b and gpt-oss-120b (OpenAI, 2025). DeepSeek-V3 (DeepSeek-AI, 2024) is the non-thinking baseline. On H-ARC, DeepSeek-R1, GLM-4.5-Air-FP8, gpt-oss-120b, and Qwen-QwQ-32B each contribute at least 298 observations. gpt-oss-20b has $n = 119$ parseable trials. Qwen3-235B-Thinking has $n = 43$ trials with four errors. These two H-ARC cells are reported descriptively. All six thinking LRMs are included in the INTUIT and Cortes analyses.

For thinking LRMs, deliberation t is the `reasoning_token_length` field in the released dataset. It records the number of intermediate-trace tokens generated before the final answer using each model's native tokenizer. For DeepSeek-V3, we use `total_output_tokens`. These quantities are treated as behavioural measures of generated duration under nominally greedy decoding. Their relation to latent computation is a subject of ongoing debate (Valmeekam et al., 2025, Samineni et al., 2025, Kambhampati et al., 2025). We standardize outcome contrasts within each agent and estimate regression coefficients on logged duration, so the comparison concerns relative changes within each system. Following de Varda et al. (2025)'s analysis script, we retain one (item, model) row from the released dataset and keep the first attempt. For cross-item duration correlations, model token counts are matched to item-level human reaction times irrespective of whether the model's final answer can be scored. Analyses involving correctness use only scored answers. INTUIT traces are restricted in the public release, so trace-content analyses use H-ARC and Cortes. SI-3 summarises provenance and scoring. The analysis code and complete per-model attempted, parseable, correct, and wrong counts are in the OSF deposit.

Paradigm	Cognitive domain	Human data	LRM data
H-ARC	Visual abstraction	400 items, 4,091 trials	5 thinking LRMs in the d-ratio summary, 6 in the per-LRM item-FE regressions[a]
INTUIT	Intuitive physics	144 items, 1,536 trials	6 thinking LRMs with both outcomes
Cortes	Relational reasoning	86 items, 20,052 trials	6 thinking LRMs (5–8 wrong trials each)
Arithmetic	Parametric arithmetic	168 items, 1,680 trials	all LRMs at ceiling (excluded)

Table 1. Datasets analysed. [a] gpt-oss-20b has $n = 119$ parseable trials, and Qwen3-235B-Thinking has $n = 43$ matched items with four wrong trials. Full dataset and scoring detail are in the OSF deposit.

Outcome-conditioned allocation and difficulty control. For agent A, paradigm P, and trial i, let $t_i > 0$ denote deliberation and $c_i \in \{0, 1\}$ denote correctness. The per-agent d-ratio is Cohen's d on log deliberation using the pooled standard deviation. Here t_i is reaction time in seconds for humans, `reasoning_token_length` for thinking LRMs, and total output length for DeepSeek-V3.

$$d_{\text{wrong}-\text{right}}(A, P) = \frac{\bar{\ell}_{\text{wrong}} - \bar{\ell}_{\text{right}}}{s_{\text{pooled}}}, \qquad \ell_i = \log t_i.$$

Positive values indicate longer deliberation on trials that end in an incorrect answer. We report a model d-ratio only when at least five correct and five incorrect trials are available.

The per-agent d-ratio combines between-item difficulty with differences between successful and failed attempts. Harder items can take longer and fail more often. Duration can also differ by outcome among attempts on the same item. We separate these sources with item fixed effects. The combined specification is

$$\log t_i = \alpha + \beta c_i + \beta_{\text{LRM}}\, c_i \times \text{LRM}_i + \delta_{\text{agent}} + \gamma_{\text{item}} + \varepsilon_i.$$

Here LRM_i equals one for model observations and zero for human trials. The interaction β_{LRM} is the LRM outcome-conditioned slope minus the human slope, with shared item effects. We also fit human-only and LRM-only item fixed-effects models, single-LRM versions of the combined regression, the same specifications on INTUIT and Cortes, and a within–between re-parameterisation (Mundlak, 1978) using item-level mean correctness in place of item dummies. Standard errors are cluster-robust by item throughout.

These coefficients relate duration to observed correctness. The human slope compares trials on the same item across the sampled population, whose participant identifiers are absent from the release. Each LRM contributes one observed outcome per (item × model) pair, so the pooled LRM slope is identified by variation across models attempting the same item. Repeated stochastic samples from one model are unavailable. Separate subgroup fits give each group its own item effects. Further specification details are in SI-2 and SI-5.

For H-ARC sensitivity analyses, we fit $\log t \sim c_c + \text{LRM} + c_c \times \text{LRM}$ with centred correctness, an LRM indicator, and an item random intercept. We also fit crossed random effects and cluster-robust OLS specifications clustered by agent and by item (Table S4). The item fixed-effects estimate with item-clustered standard errors is the primary difficulty-controlled estimand.

Trace-content analysis. For each LRM trial on H-ARC and Cortes, we compute four length-normalised features from the released `reasoning_trace`. These are self-doubt or hedge markers per 1,000 characters (`wait`, `actually`, `hmm`, `let me reconsider`, ...), self-correction markers (`scratch that`, `ignore that`, ...), word-level 5-gram repetition rate, and type–token ratio. For each feature we fit

$$\text{feature} \sim \text{correct} + \log w + C(\text{agent}) + C(\text{item}),$$

where w is trace length in words. Standard errors are cluster-robust by item. Full marker lists and the parser are in the OSF deposit. SI-4 reports the treatment of multiple comparisons.

3 Results

Across the five thinking LRMs with reported d-ratios, trace length correlates positively with human reaction time across H-ARC items, with Spearman $\rho = 0.16$–0.30 and $p < .001$. DeepSeek-V3 has $\rho = -0.05$ (Figure 1). Alongside this cross-item correspondence, all five thinking LRMs with estimable d-ratios have $d > 0$, whereas the matched human sample has $d = -0.10$. Problems that elicit more deliberation from humans tend to elicit longer thinking-model traces, yet the systems differ in whether longer attempts end successfully.

3.1 The allocation gap on H-ARC

H-ARC, the visual abstraction task, provides the primary inferential test and the largest matched model sample. Every thinking LRM with an estimable H-ARC contrast has higher mean log duration on wrong trials. Among the four model samples with at least 298 observations, Cohen's d ranges from 1.47 to 3.13. The matched human sample has $d = -0.10$ (Figure 2a and Table S1).

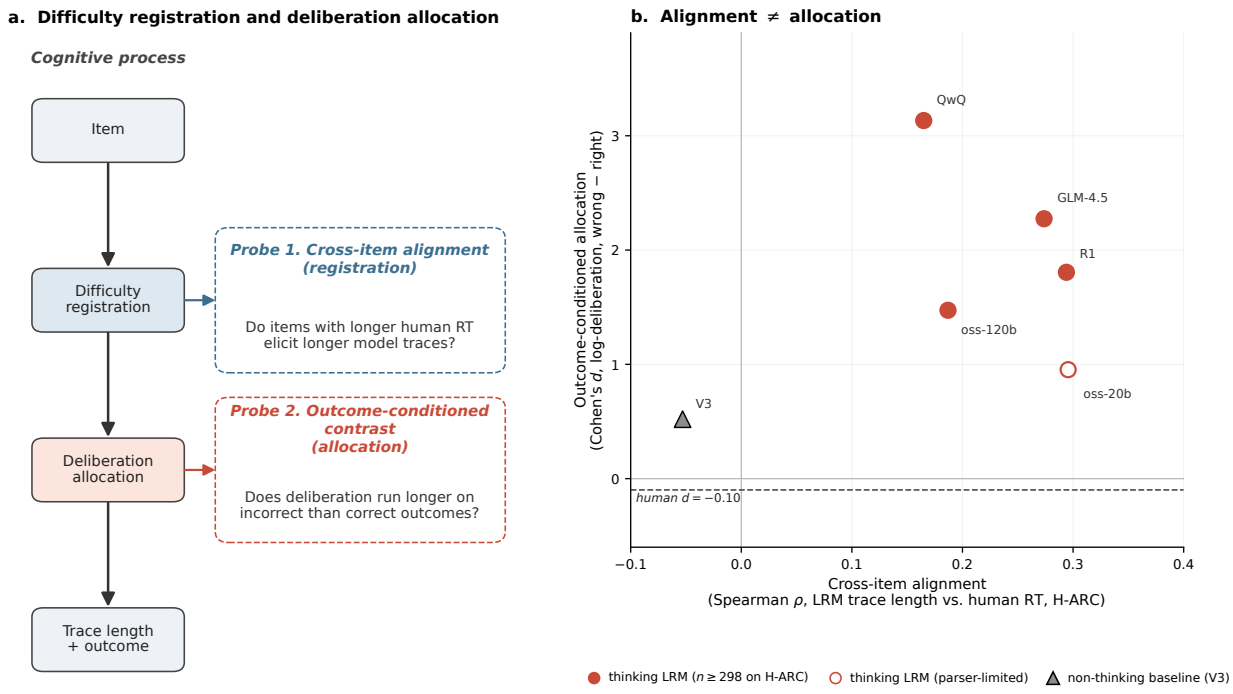

Figure 1. **Difficulty registration and deliberation allocation.** (a) Difficulty registration describes how duration varies across items. Deliberation allocation describes how duration relates to outcome. (b) H-ARC results. The horizontal axis is the cross-item Spearman ρ between LRM reasoning-token length and human reaction time. The vertical axis is per-agent Cohen's d on log deliberation (wrong − right). The open circle marks gpt-oss-20b. Its cross-item correlation uses 400 duration pairs, while its d-ratio uses 119 scored outputs. The dashed line marks the matched human $d = -0.10$, and the triangle marks non-thinking DeepSeek-V3.

The pooled descriptive means in Figure 2b point in the same directions. On wrong trials, mean human log reaction time is 0.08 lower and mean LRM log trace length is 0.78 higher than on right trials. The pooled means are plotted on separate axes. We test the human-LRM difference using item-controlled outcome slopes.

The cross-system difference remains after controlling item identity. The primary item fixed-effects model gives an agent-type × correctness interaction of $\beta_{\text{LRM}} = -0.66$ log units ($p < .001$, 95% CI $[-0.81, -0.50]$, $n = 5{,}728$). In this joint model, successful human attempts last longer than failed attempts on the same item, while failed attempts have longer traces in the pooled LRM analysis. The interaction measures the difference between these slopes. Both systems can spend longer on harder problems while differing in whether their longer attempts succeed. Controlling item identity makes this difference visible.

Four sensitivity specifications give estimates from -0.66 to -0.94, with all 95% CIs below zero (Figure 2c and Table S4). The within–between re-parameterisation (Mundlak, 1978) gives $\beta_{\text{LRM}} = -0.79$ ($p < .001$). Within-item and between-item slopes differ at $p < .001$ in both agent groups (Table S2). LRM d-ratios are also positive in nearly every difficulty quartile (SI-7, Figure S1). Collapsing repeated human trials to item×correctness cells gives $\beta_{\text{LRM}} = -0.66$ with cell-size weighting and -0.61 without weighting (SI-2).

DeepSeek-V3 also produces longer outputs on errors despite lacking an explicit thinking trace. On Cortes it has $d = 1.41$ (95% CI $[1.06, 1.84]$). Its H-ARC estimate is $d = +0.52$ with a 95% bootstrap CI of $[-0.22, +1.24]$, based on only 18 correct trials (4.5% accuracy). INTUIT accuracy is too close to floor for an estimable contrast. On H-ARC, the estimated wrong-right duration contrast is positive despite a cross-item correlation of $\rho = -0.05$ with human reaction time. The clearer Cortes result shows that error-associated expansion also occurs in ordinary generation.

3.2 Allocation across reasoning tasks

On INTUIT, every analysed thinking LRM has a positive d-ratio ($d = 0.59$–1.42 across six models), compared with $d = +0.07$ for humans. The item-controlled interaction is $\beta_{\text{LRM}} = -0.41$ ($p < .001$). The separately fitted human slope is positive ($+0.10$, $p = .087$) and the pooled LRM slope is negative (-0.33, $p = .013$). Their directions follow the H-ARC pattern, with the significant interaction providing the evidence for a cross-system difference (Figure 3).

Cortes, the binary relational-reasoning task, shows a different relation between duration and outcome. Marginally, every thinking LRM has longer traces on wrong trials ($d = 0.82$–1.96), compared with a human d-ratio of -0.31. When humans and LRMs are fitted separately with their own item effects, the pooled LRM correctness slope is $+0.31$ and the human slope is $+0.42$. Both slopes are positive. Fitting the groups together with shared item effects gives a negative agent-type interaction of $\beta_{\text{LRM}} = -0.97$ ($p < .001$).

The Cortes samples also differ between fits. The human-only fit contains 86 items, while the model and joint fits contain 58. Within the joint fit, subtracting the human slope of $+0.47$ from the LRM slope of -0.50 gives the interaction of -0.97 (SI-5). Each model has only 5–8 errors. Bootstrap intervals for the marginal d-ratio nevertheless lie above zero for all six thinking LRMs (Figure S2), and each single-LRM joint interaction is negative (Table S6). Thus the cross-system contrast extends to Cortes, while the opposite signs in the separate subgroup fits do not.

3.3 Human engagement and the form of failed model traces

Human grid edits and model trace content allow us to examine what happens during longer attempts (Figure 4).

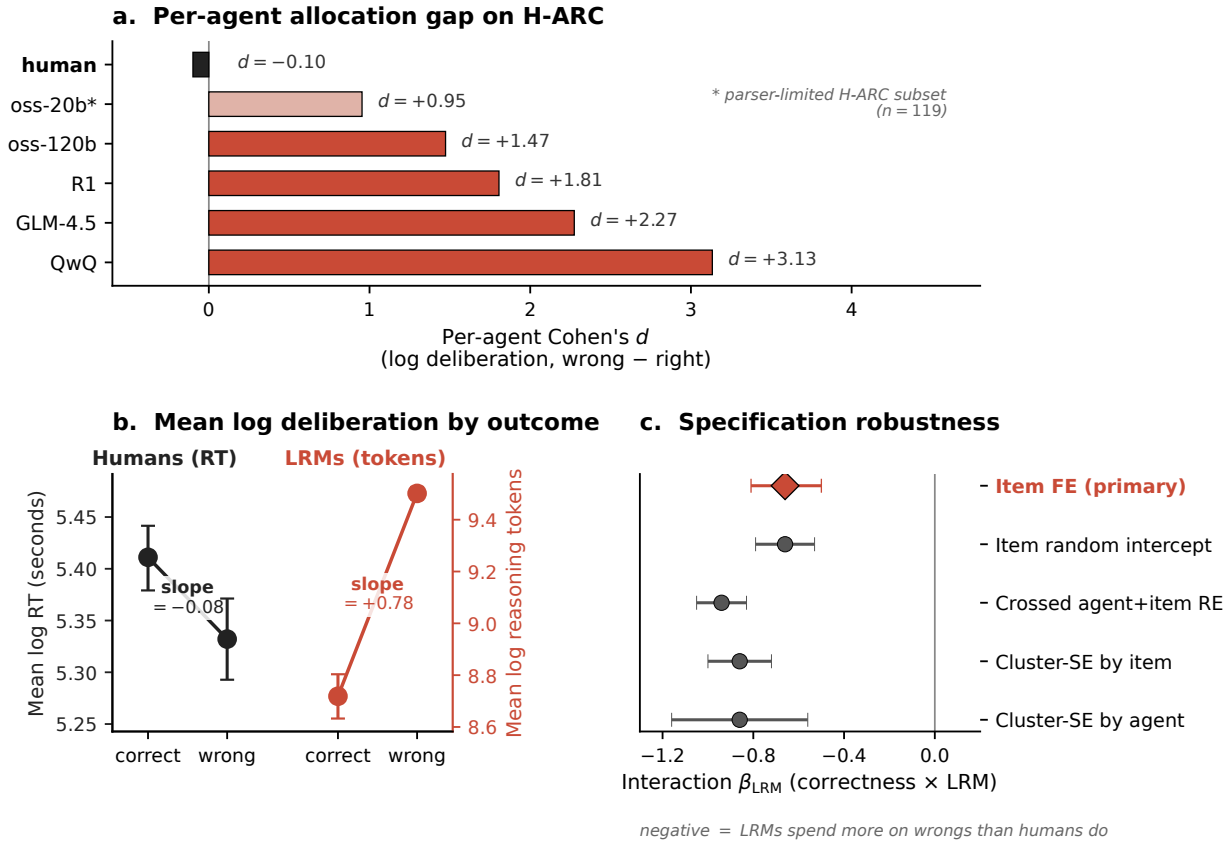

Figure 2. **The allocation gap on H-ARC.** (a) Per-agent Cohen's d on log deliberation (wrong − right). The asterisk marks gpt-oss-20b, for which 119 H-ARC outputs are parseable. Qwen3-235B-Thinking is omitted because only four H-ARC trials are wrong. Its item-FE interaction is reported descriptively in Table S1. (b) Estimated marginal mean log deliberation by outcome with bootstrapped 95% CIs. Human RT and LRM reasoning tokens use separate y-axes. Their raw levels are not directly comparable. (c) Interaction estimates across sensitivity specifications. The diamond is the primary item-fixed-effects estimand (Table S4).

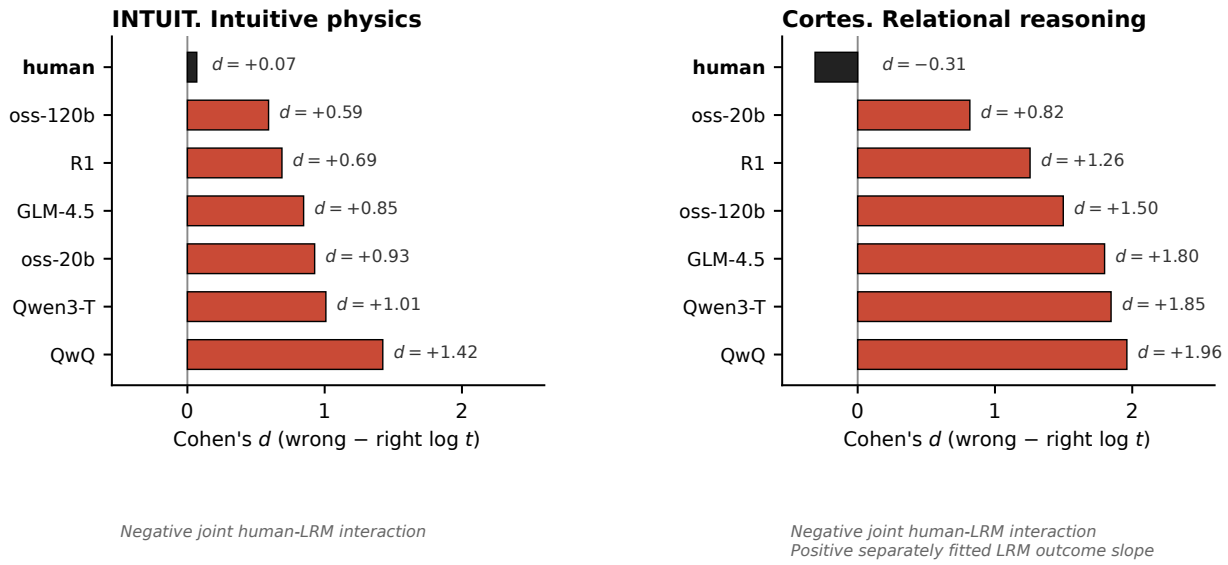

Figure 3. **Cross-paradigm allocation gap.** Per-agent Cohen's d on log deliberation (wrong − right) for the two non-saturated paradigms beyond H-ARC. INTUIT (intuitive physics) is the cross-paradigm replication. Cortes (binary relational reasoning) tests how the allocation contrast changes with the task. The combined agent-type interaction is negative in both paradigms. On Cortes, the separately fitted pooled LRM slope is positive. H-ARC is the primary analysis and is shown in Figure 2a.

For humans on H-ARC, the marginal d-ratio is close to zero at $d = -0.10$. The item-controlled correctness slope is +0.24 log units. The two quantities differ because within-item and between-item associations point in opposite directions. Within an item, solved trials are longer. Across items, easier problems are faster and more likely to be solved. At the item level, mean first-attempt reaction times yield $d = +0.60$ when items with released accuracy at or below 50% are compared with those above it. The Mundlak decomposition gives a within-item slope of +0.24 and a between-item slope of −0.54 (Table S2).

Among wrong H-ARC trials, the fastest quartile has a median of 16 grid edits and the slowest has 79. Adding log(1 + actions) to the item-controlled regression reduces the correctness slope from +0.241 to +0.125 (Figure 4a). Part of the extra time on successful attempts is thus associated with more grid activity. The action records also show that substantial work can end in failure. Short failures with few edits and long failures with many edits are consistent with selective persistence, in which some attempts end early and others sustain work without reaching a solution.

The estimated within-item correctness slope is larger on the hardest items ($\beta_{\text{correct}}^{\text{human}} = +0.32$, $p < .001$) than on the easiest quartile (+0.13, $p = .054$). Across the 341 items with both outcomes, greater reaction-time dispersion is associated with larger correctness slopes (Spearman $\rho = +0.27$, $p = 5 \times 10^{-7}$). This last association is descriptive because both quantities are derived from the same reaction-time distribution.

After controlling trace length, item, and model, wrong H-ARC traces contain 0.43 more self-doubt or hedge markers per 1,000 characters than right traces ($\beta_{\text{correct}} = -0.435$, $p = 7 \times 10^{-4}$). The unadjusted wrong-right difference has the same direction in all five models with estimable H-ARC contrasts. On Cortes, wrong traces have a 7.4 percentage-point higher 5-gram repetition rate ($\beta = -0.074$, $p = 7 \times 10^{-8}$) and a 4.1 percentage-point lower type–token ratio ($\beta = +0.041$,

$p = 10^{-3}$). The unadjusted differences in both features have the same direction in all six models.

We use *length-on-uncertainty* for longer failed traces accompanied by differences in hesitation or revisiting that remain after trace length is controlled. H-ARC failures express more explicit hedging, while Cortes failures contain more repetition and less lexical diversity.

The human records distinguish failures with little activity from failures after sustained work. The model traces show that longer failures also contain more hedging or repetition, with differences that remain after length is controlled. The process measures connect the duration contrasts to the activity sustained during an attempt, making selective human engagement and the form of extended model failures part of the allocation comparison.

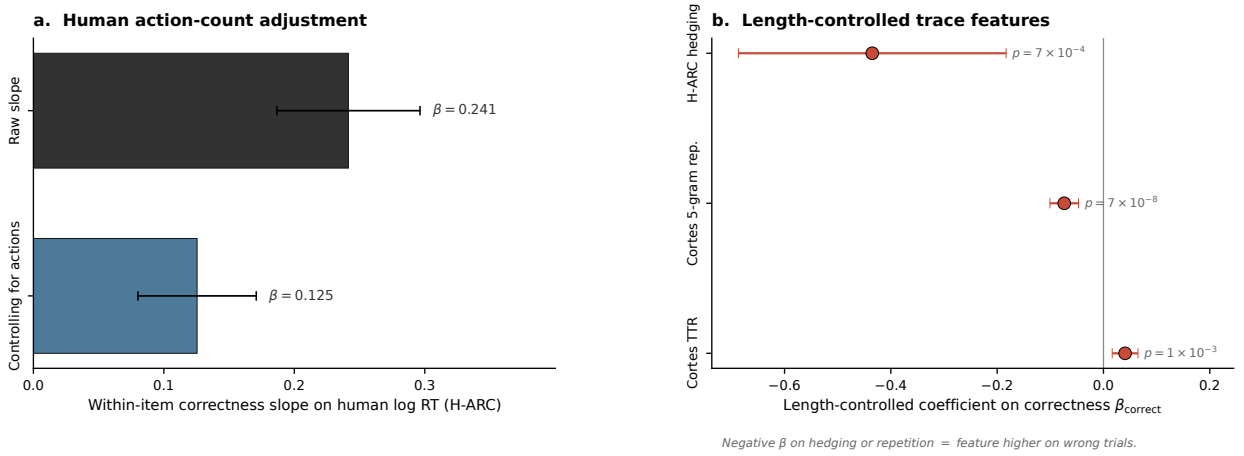

Figure 4. **Within-system behavioural probes.** (a) Human action-count adjustment. The unadjusted item-controlled correctness slope on H-ARC human log RT is $\beta = +0.241$. Adding log(1+actions) (the per-trial grid-action count) reduces it to $\beta = +0.125$, a 48% reduction. (b) LRM trace-content asymmetries. Length-controlled coefficients on correctness for the three emphasised feature×paradigm cells of Table S7. TTR denotes type–token ratio. Negative β on hedging or repetition means the feature is *higher* on wrong trials.

4 Discussion

4.1 From difficulty registration to control

On H-ARC, problems that take humans longer also tend to elicit longer model traces. Yet on the same item, successful human attempts last longer, whereas failed model attempts have longer traces in the pooled LRM analysis. The cross-problem correspondence therefore coexists with a difference in how continued work is allocated within those problems. All three tasks show a cross-system difference in the joint regression, although that difference takes different forms. The separate subgroup fits yield opposite outcome slopes on H-ARC and INTUIT, and positive slopes for both groups on Cortes.

Some human H-ARC failures involve few grid operations, while others follow substantial active work. Successful attempts on the same problem are longer on average, and action-count adjustment links part of this extra time to engagement. The selective-persistence interpretation accommodates both early endings and continued work that still fails. Across problems, however, easier items are solved more often and more quickly. These opposing relationships leave the marginal human d-ratio close to zero. The aggregate comparison can therefore suggest little difference between success and

failure even when duration is systematically related to both item difficulty and the work sustained within an attempt.

Failed model traces are longer overall, and their content also differs from successful traces at comparable length. H-ARC failures contain more explicit hedging, while Cortes failures contain more repetition. *Length-on-uncertainty* thus takes different observable forms across the two tasks. Continued search through unresolved alternatives provides an account of their shared persistence, since it can produce hesitation as well as returns to earlier material.

DeepSeek-V3 produces longer outputs on Cortes errors despite having no explicit thinking trace, showing that error-associated expansion can also occur in ordinary generation. Comparisons across training regimes can determine whether reasoning-specific training amplifies this expansion or changes its lexical expression and relation to accuracy.

In metacognitive theories, confidence and uncertainty supply information about ongoing cognition, while control determines what the system does with it (Nelson and Narens, 1990, Yeung and Summerfield, 2012, Nelson and Leonesio, 1988). Difficulty registration is broader than monitoring as used in these theories. It is defined behaviourally and can be measured without an explicit confidence report. Human confidence and model representations could differ substantially while producing a similar ordering of problems by duration. Allocation asks whether sensitivity to those problems also has comparable consequences for continued work. Human actions and model traces allow this comparison to include the work performed during deliberation.

Sequential-sampling models express the issue through the joint dependence of response time on an evidence state and a stopping rule. Resource-rational metareasoning asks what another step from that state is expected to achieve. This shifts the explanatory question from how difficult a problem is to what progress remains possible during an attempt. A demanding problem can still offer a promising next step, while an unresolved problem can cease to offer a useful direction for search. Humans and models could thus respond to the same difficulty yet continue for different lengths of time because they expect different returns from further work.

4.2 A resource-rational account and causal test

Resource-rational analysis gives deliberation allocation an explicit value criterion (Lieder and Griffiths, 2020, Gershman et al., 2015, Callaway et al., 2022). Following Russell and Wefald (1991), let s_t denote the agent's state after t units of deliberation and let $V(s_t)$ be the expected utility of the best answer available in that state according to the agent's objective. The marginal value of another unit is

$$\mathrm{mVOC}(s_t) = \mathbb{E}[V(s_{t+1}) - V(s_t) \mid s_t] - \kappa,$$

where $\kappa > 0$ is the marginal cost of computation. Continuation is favoured when the expected improvement from another unit exceeds its cost. Difficulty affects continuation through what it implies about expected improvement and cost. Similar difficulty can support different actions when the expected reducibility of uncertainty or the value of further progress differs (Zhu and Griffiths, 2025).

Agents facing similar difficulty may differ in whether they expect further work to resolve their uncertainty. Another computation may reveal useful structure, eliminate a plausible alternative, or bring a candidate answer closer to resolution. When further search seems unlikely to change the answer, the expected return falls. Distinguishing uncertainty from its reducibility (Der Kiureghian and Ditlevsen, 2009) helps interpret why human failures can be either quick or prolonged. A quick failure can follow a judgement that further work has little value. A slow failure can follow sustained work that was worthwhile in expectation but unsuccessful in outcome. Correct trials may be long because continued search sometimes reaches a solution.

For an LRM, continued search offers an explanation of the combination of long failed traces and repeated hesitation or revisiting. A policy that treats unresolved alternatives as promising directions for further work continues to generate candidate answers even on attempts that eventually end in error. In this account, the model's persistence follows the prospect of further progress, while eventual correctness records whether that search succeeded.

Even if humans and models expected the same accuracy gain from another computation, they could value it differently. The objective represented by $V(s_t)$ determines what counts as progress. For humans, solving the item competes with costs of time and effort. If a learned generation policy values properties of the output trajectory beyond final-answer accuracy, further generation can retain value even when its marginal accuracy benefit is small.

Longer human H-ARC trials contain more overt grid activity, while additional model text may include repetition, restatement, or reconsideration without a corresponding change in answer quality. Duration therefore records the continuation of different activities in the two systems. The allocation comparison captures how each system distributes that activity across attempts. Its relation to effective computation depends on how much of the continued activity can change the answer. When additional text contributes little to that change, a large expansion in visible deliberation can accompany a small increase in effective computation.

If perceived reducibility drives the gap, changing the prospect that further search can resolve uncertainty should change allocation. Where the systems value different properties of a trajectory, the gap can persist even when extra computation brings little accuracy gain. A weak relation between visible duration and effective computation would allow large trace expansions to coexist with early performance plateaus.

On Cortes, successful attempts are longer in both separate subgroup fits, and the joint model identifies a human-LRM difference under shared item effects. H-ARC and INTUIT give opposite outcome slopes in the separate fits. Together, the tasks show that an allocation difference can persist as the relationship between continued work and success changes. A control account based on expected progress accommodates successful attempts being longer in both systems when continued search offers a route to resolution.

H-ARC requires constructive search over possible transformations and permits substantial grid interaction before a final answer. INTUIT requires reasoning about physical outcomes in a structured scene. Cortes has a binary answer space and few model errors. Search space, opportunities for overt work, and the evidence of progress vary together across these tasks. Manipulating them separately would test whether allocation follows the expected reducibility of uncertainty and identify which differences account for the Cortes pattern.

A randomized reasoning-budget experiment would provide a direct causal test on the model side. Repeated samples from the same model-item pairs could be assigned different token budgets under a common forced-answer protocol, following Hu (2026). The target estimand, with B denoting the assigned token budget, is

$$p(\text{correct} \mid \text{do}(B = b), \text{model}, \text{item}).$$

Holding model and item fixed, the intervention estimates how performance changes when the opportunity for further computation is externally varied. It connects the observed distribution of longer and shorter traces to the accuracy gained from an assigned budget.

A rise in accuracy across larger budgets would show that additional available computation improves performance over that region. If this occurs where failed traces also expand, persistence can be productive in expectation even when particular trajectories end in error. An early accuracy plateau alongside continued trace expansion would instead show weak coupling between visible persistence and accuracy gains. Comparing these curves across items and tasks would reveal where

the return to further computation changes.

Measuring trace form at each budget would show whether experimentally constraining persistence changes the hedging and revisiting associated with failure. The performance curves would estimate the accuracy gained from additional available computation, while the traces would show how that opportunity is used. Combining these responses with evidence about what the generation policy rewards would connect the objectives represented by $V(s_t)$ to observable deliberative control.

4.3 Limitations

The released data support comparisons across attempts. Each model contributes one outcome per item, and the human trials lack participant identifiers. The item-controlled coefficients therefore describe population-level associations between duration and outcome. Repeated model samples and identified human trajectories would permit analysis of individual stopping rules. The proposed budget experiment addresses the effect of additional available computation.

The duration measures record different mixtures of activity. Human reaction time combines several processes (Ratcliff and McKoon, 2008, Heitz, 2014, Bogacz et al., 2006), and reasoning traces imperfectly reflect latent model computation (Valmeekam et al., 2025, Kambhampati et al., 2025, Samineni et al., 2025). Logging duration makes the slopes interpretable as within-system relative changes. Their interaction compares these relative outcome differences across systems.

The sample covers six open-weight thinking LRMs from four organisations and one non-thinking baseline. Closed-frontier systems remain outside the comparison. H-ARC and INTUIT provide the clearest opposite-sign subgroup patterns, while Cortes combines a small number of model errors with a different pattern in the separate fits. Extension to other tasks and systems should test which features of the present allocation difference recur and which depend on the search opportunities each task affords.

5 Conclusion

Thinking LRMs can track which problems take humans longer while distributing continued deliberation differently across successful and unsuccessful attempts. On H-ARC, cross-item duration alignment accompanies an item-controlled human-LRM allocation gap. INTUIT extends the gap to intuitive physics. Cortes preserves a negative joint interaction while giving positive slopes in separate subgroup fits. These results locate similarity in sensitivity to problem difficulty alongside a difference in the allocation of continued work.

Human grid actions connect longer attempts to sustained work, including on attempts that fail. Failed model traces are longer overall and contain more hedging or repetition even after length is controlled, with the form of the difference varying across tasks. The resource-rational account explains how such patterns arise when agents differ in what they expect further work to resolve, how they value progress, or how closely visible duration reflects computation that can change the answer.

Cross-problem duration correlations measure how similarly humans and models order problems by time spent. Allocation analyses test whether continued work is organised similarly once the shared item gradient is removed. The proposed reasoning-budget experiment would take the next step by measuring how additional computation changes accuracy and trace form on the same model-item pairs. Measuring registration together with allocation makes deliberative control a distinct target of comparison between human and artificial reasoners.

Acknowledgements

We thank the authors of the de Varda et al. release for making the LRM and human reasoning data public, and the H-ARC, INTUIT, and Cortes data creators for the underlying behavioural datasets.

Declarations

Ethics. This study is a secondary analysis of publicly released, de-identified behavioural and model-output data. It involved no new participant recruitment or data collection, and no identifiable personal data were accessed.

Competing Interests. The author declares no competing interests.

Data and Code Availability. All datasets analysed in this study are public. The de Varda et al. release is at `https://osf.io/r3kum/`. H-ARC is accompanied by LeGris et al. (2025), INTUIT by Prunty et al. (2025), and Cortes is redistributed in the de Varda deposit. The full analysis pipeline and intermediate results are openly available at osf.io/jxb4a. The repository includes pinned dependencies, the deterministic random seed (`0xA12C`), and a `Makefile` target that reproduces the reported results from the public source data.

References

Binz, M. and Schulz, E. (2023). Using cognitive psychology to understand GPT-3. *Proceedings of the National Academy of Sciences*, 120(6):e2218523120.

Bogacz, R., Brown, E., Moehlis, J., Holmes, P., and Cohen, J. D. (2006). The physics of optimal decision making: A formal analysis of models of performance in two-alternative forced-choice tasks. *Psychological Review*, 113(4):700–765.

Callaway, F., van Opheusden, B., Gul, S., Das, P., Krueger, P. M., Griffiths, T. L., and Lieder, F. (2022). Rational use of cognitive resources in human planning. *Nature Human Behaviour*, 6(8):1112–1125.

Chollet, F. (2019). On the measure of intelligence. *arXiv preprint arXiv:1911.01547*.

Cortés, R. A., Weinberger, A. B., Colaizzi, G. A., Porter, G. F., Dyke, E. L., Keaton, H. O., Walker, D. L., and Green, A. E. (2021). What makes mental modeling difficult? normative data for the multidimensional relational reasoning task. *Frontiers in Psychology*, 12:668256.

de Varda, A. G., D'Elia, F. P., Kean, H., Lampinen, A., and Fedorenko, E. (2025). The cost of thinking is similar between large reasoning models and humans. *Proceedings of the National Academy of Sciences*, 122(47):e2520077122.

de Varda, A. G., D'Elia, F. P., Kean, H., Lampinen, A., and Fedorenko, E. (2026a). Reply to Dujmović: The alignment in cost between human and model reasoning is an empirical phenomenon worth explaining. *Proceedings of the National Academy of Sciences*, 123(4):e2536153123.

de Varda, A. G., D'Elia, F. P., Kean, H., Lampinen, A., and Fedorenko, E. (2026b). Reply to Vankov et al.: Reasoning traces are linked to accuracy and capture key dimensions of problem complexity. *Proceedings of the National Academy of Sciences*, 123(12):e2603574123.

DeepSeek-AI (2024). DeepSeek-V3 technical report. *arXiv preprint arXiv:2412.19437*.

Der Kiureghian, A. and Ditlevsen, O. (2009). Aleatory or epistemic? Does it matter? *Structural Safety*, 31(2):105–112.

Dujmović, M. (2026). No deep insights into the alignment between human and deep learning reasoning processes: Thoughts on de Varda et al. (2025). *Proceedings of the National Academy of Sciences*, 123(4):e2533685123.

Efron, B. and Tibshirani, R. J. (1993). *An Introduction to the Bootstrap*. Chapman & Hall.

Gershman, S. J., Horvitz, E. J., and Tenenbaum, J. B. (2015). Computational rationality: A converging paradigm for intelligence in brains, minds, and machines. *Science*, 349(6245):273–278.

Guo, D., Yang, D., Zhang, H., Song, J., Wang, P., Zhu, Q., Xu, R., Zhang, R., Ma, S., Bi, X., Zhang, X., Yu, X., Wu, Y., Wu, Z. F., Gou, Z., Shao, Z., Li, Z., Gao, Z., Liu, A., et al. (2025). DeepSeek-R1 incentivizes reasoning in LLMs through reinforcement learning. *Nature*, 645(8081):633–638.

Heitz, R. P. (2014). The speed-accuracy tradeoff: History, physiology, methodology, and behavior. *Frontiers in Neuroscience*, 8:150.

Hu, Y. (2026). "Thinking traces" in large reasoning models: Cognitive cost or performative scaffolding? *Proceedings of the National Academy of Sciences*, 123(17):e2604554123.

Kambhampati, S., Valmeekam, K., Bhambri, S., Palod, V., Saldyt, L. P., Stechly, K., Samineni, S. R., Kalwar, D., and Biswas, U. (2025). Position: Stop anthropomorphizing intermediate tokens as reasoning / thinking traces! *arXiv preprint arXiv:2504.09762*.

Kojima, T., Gu, S. S., Reid, M., Matsuo, Y., and Iwasawa, Y. (2022). Large language models are zero-shot reasoners. *Advances in Neural Information Processing Systems*, 35:22199–22213.

LeGris, S., Vong, W. K., Lake, B. M., and Gureckis, T. M. (2025). A comprehensive behavioral dataset for the Abstraction and Reasoning Corpus. *Scientific Data*, 12:Article 1380.

Lieder, F. and Griffiths, T. L. (2020). Resource-rational analysis: Understanding human cognition as the optimal use of limited computational resources. *Behavioral and Brain Sciences*, 43:e1.

Mundlak, Y. (1978). On the pooling of time series and cross section data. *Econometrica*, 46(1):69–85.

Nelson, T. O. and Leonesio, R. J. (1988). Allocation of self-paced study time and the "labor-in-vain effect". *Journal of Experimental Psychology: Learning, Memory, and Cognition*, 14(4):676–686.

Nelson, T. O. and Narens, L. (1990). Metamemory: A theoretical framework and new findings. In Bower, G. H., editor, *Psychology of Learning and Motivation*, volume 26, pages 125–173. Academic Press.

OpenAI (2025). gpt-oss-20b and gpt-oss-120b [model cards]. Hugging Face.

Prunty, J., O'Flynn, A., Quinn, P., and Cheke, L. G. (2025). INTUIT: Investigating intuitive reasoning in humans and language models. In *Proceedings of the 47th Annual Meeting of the Cognitive Science Society*.

Qwen Team (2025). QwQ-32B and Qwen3-235B-A22B-Thinking-2507 [model cards]. Hugging Face.

Ratcliff, R. and McKoon, G. (2008). The diffusion decision model: Theory and data for two-choice decision tasks. *Neural Computation*, 20(4):873–922.

Russell, S. and Wefald, E. (1991). Principles of metareasoning. *Artificial Intelligence*, 49(1–3):361–395.

Samineni, S. R., Kalwar, D., Gangal, V., Bhambri, S., and Kambhampati, S. (2025). Local coherence or global validity? Investigating RLVR traces in math domains. *arXiv preprint arXiv:2510.18176*.

Simon, H. A. (1956). Rational choice and the structure of the environment. *Psychological Review*, 63(2):129–138.

Snell, C., Lee, J., Xu, K., and Kumar, A. (2025). Scaling LLM test-time compute optimally can be more effective than scaling model parameters. *The Thirteenth International Conference on Learning Representations (ICLR 2025)*.

Valmeekam, K., Stechly, K., Palod, V., Gundawar, A., and Kambhampati, S. (2025). Beyond semantics: The unreasonable effectiveness of reasonless intermediate tokens. *NeurIPS 2025 Workshop on Bridging Language, Agent, and World Models for Reasoning and Planning (LAW 2025)*.

Vankov, I. I., Adolfi, F., Heaton, R. F., Puebla, G., and Bowers, J. S. (2026). Correlations without causation do not support claims of human–LLM reasoning alignment. *Proceedings of the National Academy of Sciences*, 123(12):e2536362123.

Wei, J., Wang, X., Schuurmans, D., Bosma, M., Ichter, B., Xia, F., Chi, E. H., Le, Q. V., and Zhou, D. (2022). Chain-of-thought prompting elicits reasoning in large language models. *Advances in Neural Information Processing Systems*, 35:24824–24837.

Yeung, N. and Summerfield, C. (2012). Metacognition in human decision-making: Confidence and error monitoring. *Philosophical Transactions of the Royal Society B: Biological Sciences*, 367(1594):1310–1321.

Z.ai (2025). GLM-4.5-Air-FP8 [model card]. Hugging Face.

Zhu, J.-Q. and Griffiths, T. L. (2025). Computation-limited Bayesian updating: A resource-rational analysis of approximate Bayesian inference. *Psychological Review*. Advance online publication.

Supplementary Information

SI-1. Single-LRM item fixed-effects interactions on H-ARC

Table S1 reports the combined item-FE interaction after refitting the human sample with each thinking LRM separately. The four H-ARC model samples with at least 298 observations all return negative interactions at $p < 10^{-4}$. The gpt-oss-20b estimate is treated descriptively because only 119 final grids are parseable, and the Qwen3-235B-Thinking estimate is descriptive because only four of its 43 released H-ARC trials are wrong. The corresponding per-agent Cohen's d values for the estimable cells are shown in Figure 2a.

Model	n_{LRM}	n_{wrong}	β_{LRM}	95% CI	p
Qwen-QwQ-32B	400	380	-0.831	$[-1.22, -0.44]$	2.9×10^{-5}
gpt-oss-20b†	119	91	-0.815	$[-1.24, -0.39]$	1.9×10^{-4}
gpt-oss-120b	389	322	-0.808	$[-1.05, -0.57]$	5.0×10^{-11}
GLM-4.5-Air-FP8	388	356	-0.731	$[-1.00, -0.46]$	8.3×10^{-8}
DeepSeek-R1	298	237	-0.584	$[-0.75, -0.42]$	1.3×10^{-12}
Qwen3-235B-Thinking†	43	4	-0.323	$[-0.56, -0.09]$	6.4×10^{-3}

Table S1. **H-ARC single-LRM item-FE interactions** (*The allocation gap on H-ARC*). β_{LRM} is the within-item correctness-slope difference between the LRM and humans, with item fixed effects and cluster-robust SE by item. † The dagger marks descriptive estimates. gpt-oss-20b has $n = 119$ parseable final outputs. Qwen3-235B-Thinking is identified from four wrong trials.

SI-2. H-ARC robustness and alternative specifications

Within–between decomposition. The Mundlak parameterisation separates the within-item correctness slope β_W from the between-item component β_M. The between-item slope is $\beta_W + \beta_M$.

Subgroup	Within-item β_W	Between-item $\beta_W+\beta_M$	Mundlak β_M (p)
Humans only	$+0.241$	-0.535	-0.777 (5×10^{-22})
LRMs (pooled)	-0.234	-1.214	-0.980 (2×10^{-17})
Combined frame, $\beta_{\text{LRM}} = -0.793$ ($p = 8 \times 10^{-28}$)			

Table S2. **Mundlak within–between decomposition on H-ARC** (*The allocation gap on H-ARC*). The combined-frame dissociation under Mundlak (-0.79) is larger in magnitude than the primary item-FE estimand (-0.66).

Aggregation. The public release contains multiple human trials per item and omits participant identifiers. We collapse each human item×correctness cell to its mean $\log t$, once weighted by cell size and once unweighted, while leaving each LRM model×item row unchanged. Both aggregated fits reproduce the negative interaction from the trial-level model (Table S3).

Alternative specifications and identification. The item fixed-effects model with item-clustered standard errors is the primary difficulty-controlled specification. Table S4 reports four sensitivity analyses using random effects or alternative clustering. They differ in how between-item information and agent-level variation enter the fit, so their coefficient magnitudes are not interpreted as directly interchangeable. The agent-clustered OLS fit has only seven clusters and is included as a finite-cluster sensitivity analysis.

Specification	n_{obs}	β_{LRM}	SE	p	95% CI
Trial-level (primary)	5,728	−0.655	0.078	4×10^{-17}	[−0.81, −0.50]
Cell-aggregated, weighted	2,417	−0.655	0.082	2×10^{-15}	[−0.82, −0.49]
Cell-aggregated, unweighted	2,417	−0.606	0.070	4×10^{-18}	[−0.74, −0.47]

Table S3. **Aggregated-cell robustness on H-ARC.** Human trials are collapsed to (item×correctness) cells. LRM rows are left at one observation per (model×item). The combined item-FE dissociation regression is then re-estimated. Weighted by cell size or unweighted, the primary interaction coefficient is essentially unchanged from the trial-level estimate.

In the pooled LRM item-FE regression, the outcome slope is identified by variation across models attempting the same item. A single-LRM combined fit is identified by variation across the human trials and that model on the same item. The released data contain one outcome per model×item pair, so none of these regressions estimates a repeated stochastic within-item slope for one model.

Specification	Interaction β	SE	z/t	p
Item random intercept (mixed-effects anchor)	−0.660	0.054	−12.31	$< .001$
Crossed random agent + item	−0.940	0.058	−16.24	$< .001$
OLS, cluster SE by agent	−0.862	0.089	−9.67	$< .001$
OLS, cluster SE by item	−0.862	0.073	−11.77	$< .001$
Item fixed effects (primary estimand)	**−0.655**	**0.078**	**−8.42**	**$< .001$**

Table S4. **H-ARC dissociation interaction across specifications.** Centred correctness × LRM interaction. The bold row is the primary difficulty-controlled estimand (within-item identification, cluster-robust SE by item). The four upper rows are mixed-effects and cluster-robust sensitivity analyses that return the same interaction sign without imposing strict within-item identification. The agent-clustered OLS row is a finite-cluster sensitivity check with only seven clusters, the human population plus the six thinking LRMs. All five specifications agree in sign.

SI-3. LRM data provenance and scoring

The released frame (de Varda et al., 2025) contains each model's prompt, full output, final-answer fields, and token counts. For thinking LRMs we use `reasoning_token_length`, counted in the model's native tokenizer. For DeepSeek-V3 we use `total_output_tokens`. Models are not retokenized onto a common scale, and raw token counts are not compared across models. Final-answer correctness follows the parser used in the de Varda et al. analysis, augmented for H-ARC grid outputs by a regular-expression match against `Correct_answer`. Full attempted, parseable, correct, and wrong counts are provided in the OSF deposit.

gpt-oss-20b. Only 119 of 400 final grids are parseable. The remaining outputs have no correctness label, so this cell is reported descriptively. *Qwen3-235B-Thinking.* Only 43 H-ARC items appear in the released frame and four are wrong, so its H-ARC single-model estimates are also treated descriptively.

SI-4. Multiple-comparison treatment

The reported p-values are unadjusted. Treating the three combined paradigm interactions as one family, all three interactions remain significant under Bonferroni and Holm correction. Among the eight trace-content feature×paradigm tests in Table S7, the three effects used in the main-text interpretation also survive Bonferroni correction. The H-ARC type–token-ratio effect has $p \approx .0063065$, just above the Bonferroni threshold of $.05/8 = .00625$. Secondary cells not used as primary inferential evidence are treated descriptively in the text.

SI-5. Cross-paradigm item-FE regressions and single-LRM interactions

Table S5 reports the human-only, pooled-LRM, and combined item-FE regressions for H-ARC, INTUIT, and Cortes. Arithmetic is omitted because every thinking LRM solves every item. Separate subgroup fits estimate item effects within each group. The combined regression imposes shared item effects and estimates both outcome slopes jointly on items represented in both groups. Its interaction is the jointly estimated LRM slope minus the human slope. On Cortes, the human-only regression uses 20,052 trials on 86 items, the LRM-only regression uses 348 trials on 58 items, and the combined regression uses 13,888 observations on the 58 shared items. The combined human slope is +0.471 and the implied LRM slope is −0.497, yielding the interaction of −0.968. Each Cortes model contributes only 5–8 wrong trials.

			Humans only		LRMs pooled		Combined dissoc.	
Paradigm	n_{H}	n_{LRM}	β_{correct}	p	β_{correct}	p	β_{LRM}	p
H-ARC	4,091	1,637	+0.241	$< .001$	−0.271	$< .001$	−0.655	$< .001$
INTUIT	1,536	864	+0.102	.087	−0.331	.013	−0.410	$< .001$
Cortes	20,052	348	+0.418	$< .001$	**+0.310**	.001	−0.968	$< .001$

Table S5. **Cross-paradigm item-FE regressions.** Three within-item regressions per paradigm, with cluster-robust SE by item. The bold entry marks the positive LRM slope in a separate subgroup fit. Sample sizes in the first two columns refer to the subgroup fits, not necessarily the combined regression.

Table S6 reports the corresponding combined regression after pairing the human sample with one LRM at a time. Every model–paradigm interaction is negative. The limited H-ARC cells for gpt-oss-20b and Qwen3-235B-Thinking remain descriptive for the reasons given in SI-1 and SI-3.

Model	H-ARC	INTUIT	Cortes
Qwen-QwQ-32B	−0.83	−0.73	−1.51
gpt-oss-120b	−0.80	−0.27	−1.20
GLM-4.5-Air-FP8	−0.73	−0.29	−0.94
gpt-oss-20b	−0.78	−0.69	−0.77
DeepSeek-R1	−0.57	−0.14	−0.73
Qwen3-235B-Thinking	−0.27	−0.18	−0.77

Table S6. **Single-LRM interaction β_{LRM} across paradigms.** Combined regression refit on humans plus each single LRM, with item fixed effects and cluster-robust SE by item. Each fit uses items shared by the human sample and the particular LRM. On H-ARC this restriction is applied separately for each model. Table S1 retains the full human sample, including items absent from the paired model's data. The resulting differences are largest for the two limited H-ARC cells.

SI-6. Trace-content regressions

Table S7 reports all eight length-controlled feature×paradigm coefficients specified in the *Trace-content analysis* section of Methods. The three rows emphasised in the main text are shown in bold. INTUIT reasoning traces are restricted in the public release and are not included in this analysis.

Paradigm	Feature	β	SE	p	95% CI
H-ARC	Self-doubt / hedge density / 1k chars	$\mathbf{-0.435}$	0.128	7×10^{-4}	$[-0.69, -0.18]$
H-ARC	Self-correction density	-0.0018	0.0012	.15	$[-0.004, +0.001]$
H-ARC	5-gram repetition rate	$+0.016$	0.009	.09	$[-0.002, +0.034]$
H-ARC	Type–token ratio	-0.004	0.001	.006	$[-0.007, -0.001]$
Cortes	Self-doubt / hedge density / 1k chars	-0.817	0.834	.33	$[-2.45, +0.82]$
Cortes	Self-correction density	-0.0021	0.0015	.16	$[-0.005, +0.001]$
Cortes	5-gram repetition rate	$\mathbf{-0.074}$	0.014	7×10^{-8}	$[-0.10, -0.05]$
Cortes	Type–token ratio	$\mathbf{+0.041}$	0.012	10^{-3}	$[+0.02, +0.06]$

Table S7. **Trace-content regressions, length-controlled.** For each feature, β is the coefficient on correctness in feature $\sim$ correct $+ \log w + C(\text{agent}) + C(\text{item})$ with cluster-robust SE by item. A negative β on the self-doubt / hedge density or repetition row means the feature is *higher* on wrong trials. Bold rows are the emphasised content asymmetries on each paradigm. INTUIT traces are restricted in the public release.

SI-7. Additional robustness and uncertainty figures

Figure S1 collects additional H-ARC robustness checks. Figure S2 reports Cortes per-agent non-parametric bootstrap intervals (Efron and Tibshirani, 1993).

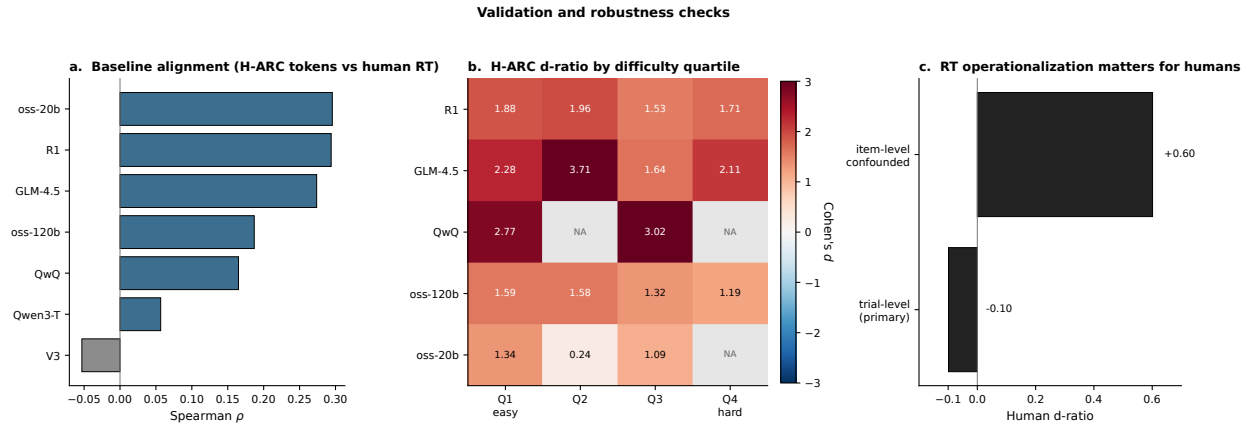

Figure S1. **Robustness checks for the H-ARC allocation gap.** (a) Cross-item Spearman correlation between LRM reasoning-token length and human reaction time on H-ARC. DeepSeek-V3 is the non-thinking baseline and shows no positive correlation. (b) LRM d-ratios by difficulty quartile. Cells marked "NA" have fewer than five right or five wrong trials, so no d-ratio is reported. (c) Human d-ratio under the trial-level (primary) and item-level operationalisations. The item-level contrast groups items by released accuracy at or below 50% versus above it.

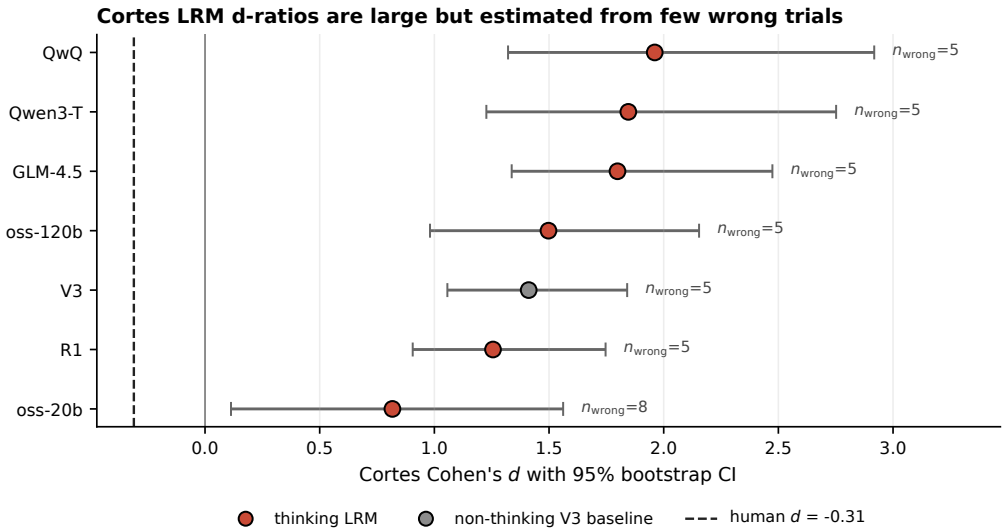

Figure S2. **Cortes bootstrap uncertainty.** Points are Cortes d-ratios per agent. Horizontal bars are 95% bootstrap confidence intervals from 10,000 resamples. Per-LRM wrong-trial counts are annotated on the right of each interval. The dashed line marks the human Cortes d-ratio. The non-thinking DeepSeek-V3 baseline is included for reference.